ELSEVIER

Chemosphere 58 (2005) 715–733

CHEMOSPHERE

www.elsevier.com/locate/chemosphere

Fluorescence fingerprint of fulvic and humic acids from varied origins as viewed by single-scan and excitation/emission matrix techniques

M.M.D. Sierra [a,*], M. Giovanela [b,c], E. Parlanti [d], E.J. Soriano-Sierra [e]

[a] *Departamento de Química, Universidade Federal de Santa Catarina, 88040-900 Florianópolis, SC, Brazil*
[b] *Centro Tecnológico (CETEC), Universidade de Caxias do Sul (UCS), 95070-560 Caxias do Sul, RS, Brazil*
[c] *Departamento de Física e Química (DEFQ), Centro de Ciências Exatas e Tecnologia (CCET), Universidade de Caxias do Sul (UCS)—95070-560 Caxias do Sul, RS, Brazil*
[d] *Laboratoire de Physico-Toxicochimie des Systèmes Naturels (LPTC), UMR 5472 CNRS, Université Bordeaux I, 351 Cours de la Libération, 33405 Talence Cedex, France*
[e] *Núcleo de Estudos do Mar (NEMAR), Universidade Federal de Santa Catarina, 88040-900 Florianópolis, SC, Brazil*

Received 18 March 2004; received in revised form 17 September 2004; accepted 23 September 2004

Abstract

Excitation/emission matrix (EEM), single-scan excitation and synchronous fluorescence spectra of a series of FA and HA from distinct environments are presented. The EEM plots show at least four spectral features whose corresponding *Ex*/*Em* pairs relate to the α′, α, β and γ (or δ) fluorophores previously found in natural waters spectra. The α′ and α peaks, which identify typical humic-like components, are present in all samples, independently of the organic matter (OM) source. In FA, their *Ex*/*Em* pairs are ~260 nm/460 nm and ~310 nm/440 nm, respectively. In HA their excitation and emission maxima are red-shifted, the corresponding *Ex*/*Em* pairs being located at ~265 nm/525 nm and ~360 nm/520 nm, respectively. The appearance of β and γ (or δ) peaks is dependent both on the OM origin and on HS aging. The former (*Ex*/*Em* ~ 320 nm/430 nm), that has been associated with the incidence of marine humic-like material, is present only in a few marine and estuarine HA. It emerges as a shoulder on the α peak and its detection is dependent on a balance between its magnitude and the magnitude and emission maxima location of the α peak. The γ (or δ) peak (*Ex*/*Em* ~ 275 nm/315 nm in FA, and ~275 nm/330 nm in HA), on the other hand, is better visualized in FA than in HA diagrams. It has typical protein-, mainly tryptophan-like, fluorescence properties and appears with varied significance in a few marine and estuarine samples being hardly detected in samples from exclusively terrestrial environments. It is also shown in this study that with selected λ_{ex}, λ_{em} and $\Delta\lambda$ values, regular emission, excitation and synchronous spectra can, together, provide a good picture of the OM sources and aging for extracted HS.

1. Introduction

Studies on humic substances (HS) structural characteristics are particularly complicated because in addition to their natural complexity they have usually been

* Corresponding author. Tel.: +55 48 331 9230; fax: +55 48 331 9711.
E-mail address: sierra@qmc.ufsc.br (M.M.D. Sierra).

0045-6535/$ - see front matter © 2004 Elsevier Ltd. All rights reserved.
doi:10.1016/j.chemosphere.2004.09.038

obtained utilizing different methods, in different laboratories, inhibiting the comparison of results. Since the establishment of the (International Humic Substances Society) IHSS procedure for HS collection (Swift, 1996), however, at least this part of the problem has been minimized and research on structural characteristics of HS has progressed considerably. Even so, most studies have focused on terrestrial, mainly soil, material, the knowledge on properties of HS from aquatic environments being less developed.

With the purpose of improving understanding vis-à-vis the structural and functional properties of HS from aquatic systems as well as of determining the relationships between these properties and the sources and evolution of organic matter (OM) within these environments, a set of fulvic (FA) and humic acids (HA) extracted from marine, estuarine, lacustrine and terrestrial environments were studied. The method utilized to extract the HS was that recommended by the IHSS (IHSS home page, 2004). Structural and spectral properties of these samples were extensively scrutinized (Fernandes et al., 2004; Giovanela et al., 2004; Sierra et al., 2004) and the data obtained supported both, the idea that HS from aquatic and mixed environments are more aliphatic and have higher nitrogen, sulphur and oxygen contents than had previously been proposed and, also, that amide linkages form important fractions of their structures. In the present work the data relative to the fluorescence properties of these samples are shown.

Knowledge on HS fluorescence properties has mostly been gained from single-scan fluorescence data. Single-scan fluorescence emission spectra of HS present a single broad band whose maximum emission (λ_{max}) shifts according to the excitation wavelength (λ_{ex}) adopted (Senesi, 1990; Sierra et al., 2000). For identical λ_{ex}, FA fluoresce with higher intensities and at shorter wavelengths than HA from the same origin (Belin et al., 1993; Sierra et al., 2000). HS excitation spectra exhibit two broad peaks positioned in the ultraviolet (around 250 nm) and visible (around 340 nm) spectral ranges. The exact localization of these peaks depends on the λ_{em} employed and the relative intensities for FA and HA are different, these also changing according to the origin of the samples (Belin et al., 1993; Sierra et al., 2000). Since in HS studies, different laboratories often use different λ_{ex} and λ_{em}, comparison between distinct studies is problematic and, for this reason, a consistent fluorescence fingerprint of HS is not yet well established.

EEM produces fluorescence spectra at many different excitation wavelengths providing an overall view of all features existing within a selected spectral range. This technique has satisfactorily been used to scrutinize water masses in natural environments (Mopper and Shultz, 1993; Coble, 1996; Mattews et al., 1996; Del Castillo et al., 1999; Mounier et al., 1999; Parlanti et al., 2000, 2002; Baker, 2001; Chen et al., 2003). A few studies on the effect of concentration, ionic strength, pH and copper binding on fluorescence features of extracted HS have also employed the EEM mode (Mobed et al., 1996; Fukushima et al., 1997). Papers on the effect of the OM origin and aging on the three-dimensional fluorescence features of HS are, however, scarce in the literature. In this study, the EEM diagrams of the HS cited above are scrutinized to establish a complete fluorescence fingerprint (i.e. number of peaks, their location and relative intensities) of this material as well as to identify potential correlations between such features and the origin of the samples. To present a deep analysis of the data and also to compare our findings to related works, a few single-scan excitation and synchronous spectra were included. For the same reasons the commercial Aldrich HA as well as soil and river FA and HA samples from the pool of standard materials of the IHSS were also included.

2. Experimental

2.1. Sampling sites

The marine sediment samples were collected from Mar Virado Island (MVI) and Ubatumirim Beach (UBM); estuarine and freshwater samples from Ratones Mangrove (RME) and Peri Lagoon (PLN). The four sampling sites are located in the southern coastal zone of Brazil, the first two being in São Paulo (zoom a in Fig. 1) and the other two on Santa Catarina Island (zooms b and c in Fig. 1).

Peri Lagoon is a freshwater lake (zoom b in Fig. 1). Three streams flow into this system, which is located in a hydrographic basin surrounded by a dense sub-tropical and well-preserved rain forest. Two sediment samples were collected at two different points from the bottom of the lake: near to the edge (PLN 4) and in the middle of the lake (PLN 7).

The Ratones Mangrove estuarine sediment samples were taken from distinct points within the estuary (zoom c in Fig. 1). One is located at the mouth of the Ratones River (RME 1) and is exposed to daily seawater washing, whereas the other (RME 2) is located far from tidal influence in a mangrove area surrounded by terrestrial vegetation. Only occasionally during exceptionally high flood tides does the RME 2A site inundate and receive marine inputs. In these two sites, sediment samples were collected at three different depths: 0–10 cm (RME 1A and 2A), 10–20 cm (RME 1B and 2B) and 20–30 cm (RME 1C and 2C).

The Aldrich HA was included as representing a material from terrestrial OM sources and also to make possible eventual comparisons with studies by other investigators. Information on the specific source and

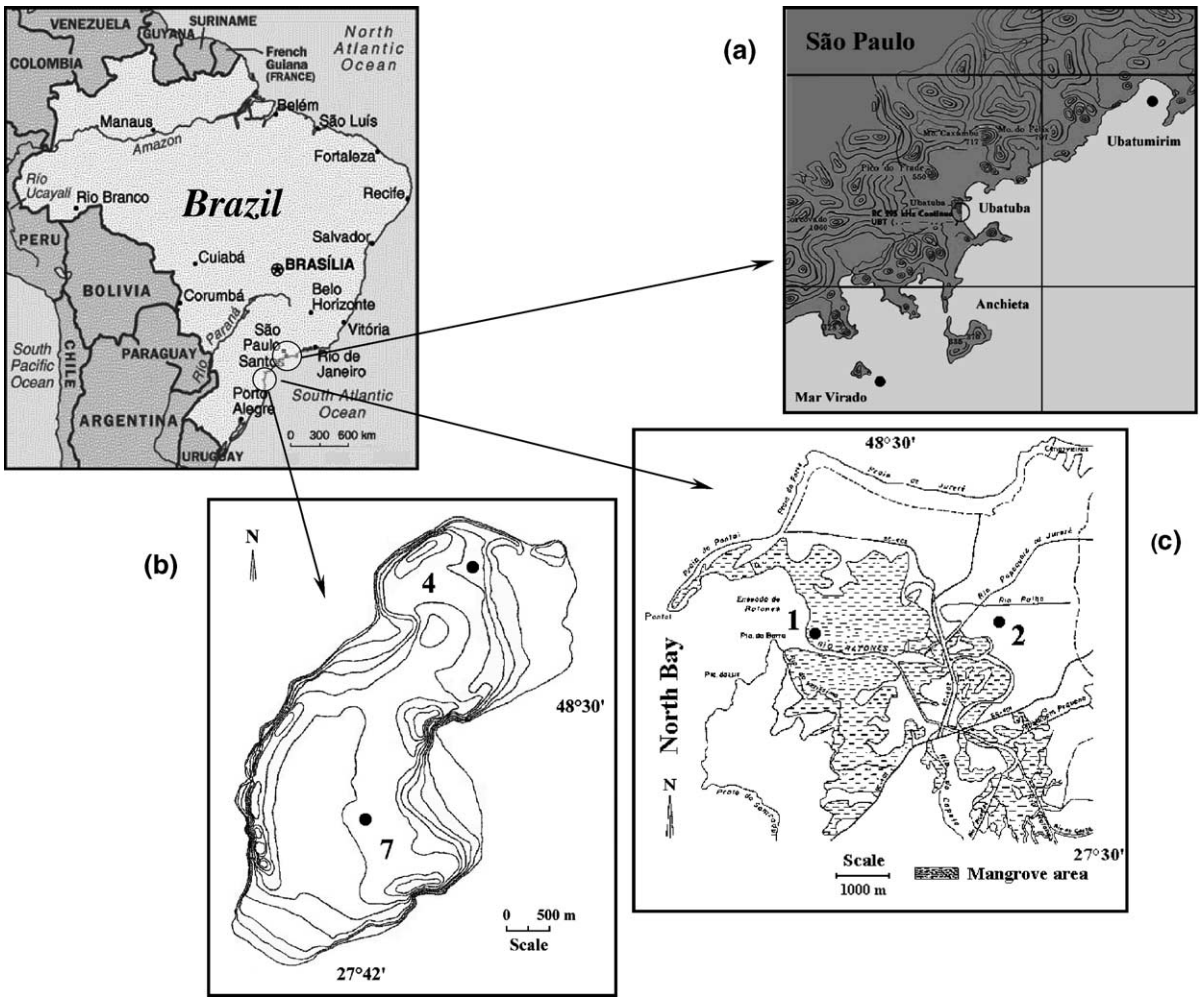

Fig. 1. Sampling sites.

nature of this product is not usually given by the suppliers, but according to Malcolm and MacCarthy (1986) this commercial HA appears to be similar to leonardite and Wyoming dopplerite and is therefore different from soil and water HS.

Four samples were purchased from the IHSS pool of standard materials, the Suwannee River FA (1S101F) and HA (1S101H), and the Elliot Soil FA (1S102F) and HA (1S102H). Complementary information on these samples can be found on the IHSS home page (2004).

2.2. Humic substances extraction procedure

All samples were obtained via the IHSS recommended procedure (Swift, 1996) and experimental details have been published elsewhere (Giovanela et al., 2004; Sierra et al., 2004). The Aldrich HA passed through the same purification process applied to the other samples.

2.3. Fluorescence spectroscopy

The fluorescence spectra of the FA and HA solutions (4 $mg l^{-1}$ of HS) were recorded with a Fluorolog SPEX FL3-22 Jobin Yvon fluorometer. Prior to analysis, the pH of the solutions was adjusted to 7.0 with 0.001 $mol l^{-1}$ NaOH. Solutions were irradiated in a 1 cm path length fused silica cell (Hellma), thermostated at 20 °C. The EEM fluorescence spectroscopy involved scanning and recording of 17 individual emission spectra (260–700 nm) at sequential 10 nm increments of excitation wavelength (λ_{ex}) between 250 and 410 nm as described elsewhere (Parlanti et al., 2000). The bandwidths for both excitation and emission were 4 nm, with emission wavelength (λ_{em}) increments of 1 nm and integration time of 0.5 s. The spectra were obtained by subtracting Milli-Q (Millipore) water blank spectra, recorded under the same conditions, to eliminate water Raman scatter peaks. The 17 scans were used to generate

three-dimensional contour plots of fluorescence intensity as a function of excitation and emission wavelengths. The emission spectra were electronically corrected for instrumental response (Ewald et al., 1983; Sierra et al., 1994) but the emission correction was not valid below 300 nm. The excitation correction was not applied to the spectra. However, the comparative discussion of emission spectra below takes into account the fact that firstly, they were recorded on the same instrument under the same experimental conditions and secondly, they did not present visible distortions relative to corrected spectra published elsewhere (Belin et al., 1993; Sierra et al., 1994).

3. Results and discussion

3.1. EEM fluorescence

The EEM fluorescence and the respective three-dimensional projections of the aqueous solutions of FA and HA samples from three different types of sediment can be seen in Figs. 2 and 3, respectively. The plots of the IHSS standard materials Suwannee River and Elliot Soil FA and HA as well as of the Aldrich HA, are shown in Figs. 4 and 5. In general terms the shape of the EEM diagrams as well as of their three-dimensional projections is basically the same for all samples studied here, with all of them presenting two main regions of different intensities. For FA, the first and more intense region is centred at *Ex*/*Em* = 260 nm/460 nm and the second, less intense, is near *Ex*/*Em* = 310 nm/440 nm. For HA, these two regions are located at around *Ex*/*Em* = 265 nm/525 nm and *Ex*/*Em* = 360 nm/520 nm, respectively. The emission maxima of the Suwannee River HA are blue-shifted and those of the Elliot Soil HA are red-shifted relatively to our HA emission maxima. Mobed et al. (1996), have previously published EEM fluorescence diagrams of the Suwannee River standard FA and HA but in their work the inspected excitation range was from 300 to 500 nm disregarding or only partially covering the short-wavelength feature (with $Ex \sim 260$ nm) found here. The second peak observed in their work, on the other hand, has *Ex*/*Em* pairs close to those found here for these samples. The *Ex*/*Em* pairs relative to these two peaks as well as those of other peaks, that will be mentioned below, for all samples studied here, are presented in Tables 1–3. Our observations extend only to $\lambda_{ex} = 250$ nm and because of this, for a few FA samples whose excitation ranges extend towards the blue-end, the α' peak is only partially registered. Such an effect does not restrain the assessment of the α' maxima wavelength values which can be clearly determined for all samples.

Considering their overall shape these EEM are similar to those of natural, mainly, fresh and pore waters (Coble, 1996; Parlanti et al., 2000; Parlanti et al., 2002; Patel-Sorrentino et al., 2002). Taking into account the *Ex*/*Em* maxima, however, a few differences can be noticed both, between extracted HS and natural water and between FA and HA plots. For natural waters, these two main peaks are located in the range *Ex*/*Em* = 250–260 nm/380–480 nm and in the range *Ex*/*Em* = 330–350 nm/420–480 nm, respectively, being consequently similar to our FA but different from our HA diagrams. The fluorophores responsible for these two signals have already been recognized as belonging to typical humic-like components, having received individual designations like as, A and C (Coble, 1996; Patel-Sorrentino et al., 2002) or, α' and α (Parlanti et al., 2000, 2002), respectively. Parlanti et al. (2000) designations will be employed in this paper.

The similarity between our FA *Ex*/*Em* pairs and those observed for natural waters confirms that this fraction of HS is chiefly responsible for natural waters fluorescence. This is to be expected since FA comprise the soluble fraction of HS. HA, on the other side, are only weakly soluble in water in the acidic and neutral pH ranges and, even when present in natural waters they might be in very low concentrations. The more soluble humic components must hence mask their fluorescence signal.

For FA, the α peak is well defined whereas for HA this signal is more like a shoulder and cannot in, most cases, be considered as a peak. In truth, if an imaginary line, parallel to the excitation axis, crosses over the two peak ranges in EEM plots at $\lambda_{em} \sim 450$ nm, it can be recognised that the second range corresponds to the second peak of a HS or natural-water single-scan corrected excitation spectrum (Belin et al., 1993; Sierra et al., 1994, 2000; Patel-Sorrentino et al., 2002). The excitation spectra so obtained of a FA and a HA are presented in Fig. 6. Moreover, whereas for FA this line crosses just over the two main peaks, generating, consequently two excitation bands, for HA, it passes away from the more featured range producing, a less featured excitation spectrum. Actually, the whole fluorescence picture given here by the EEM mode reveals that, for HA, the best emission wavelength for single-scan excitation spectra recording would be 520 nm (or close to) instead of the previously employed 445 nm (Belin et al., 1993; Sierra et al., 2000). However, even using this wavelength, the HA excitation spectra is poorly featured as can be seen in Fig. 7 confirming the reduced incidence of α type fluorophores in this humic fraction. In single-scan spectra studies, variations in the shape of this second excitation peak from one sample to another have been associated with molar mass distributions as well as with differences in the relative proportions of acidic functional groups in HS structures (Belin et al., 1993; Silva, 1996; Sierra et al., 2000). For freshwater extracts, for example, it has been shown that the higher the apparent

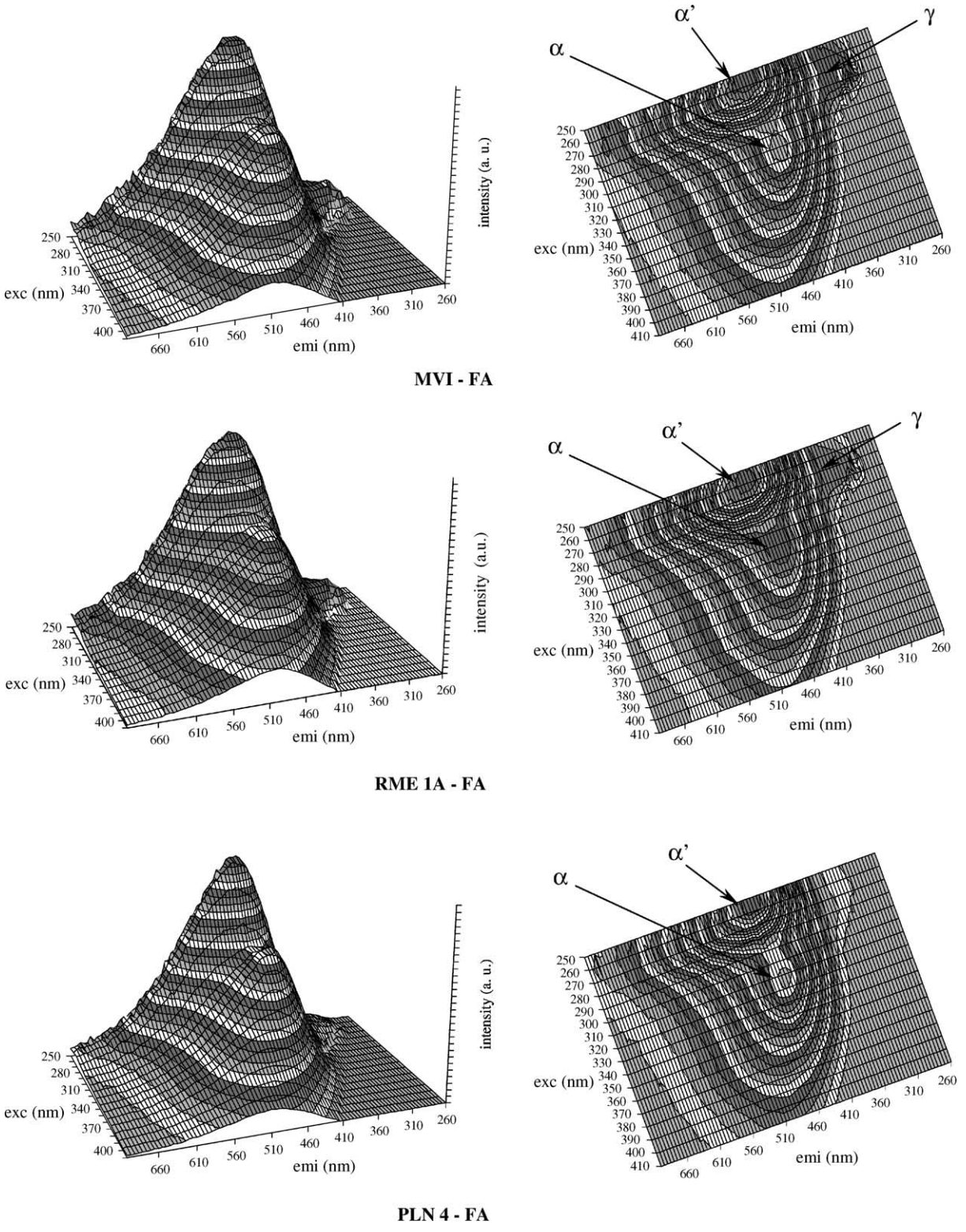

Fig. 2. EEM fluorescence diagrams and the corresponding three-dimensional projections of three FA samples. (a) MVI = coastal marine; (b) RME-1A = estuarine (near-to-sea); and (c) PLN 4 = freshwater lagoon.

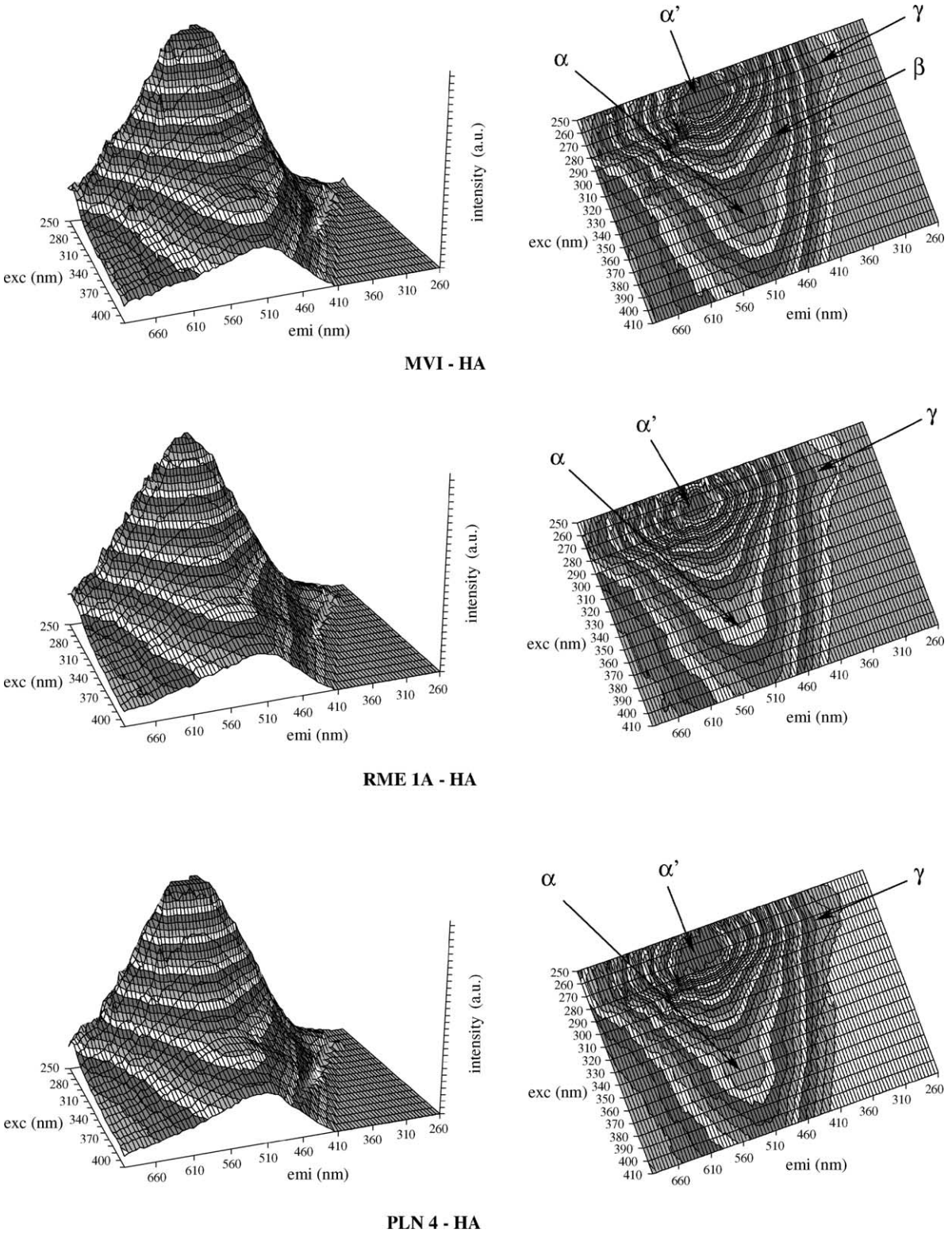

Fig. 3. EEM fluorescence diagrams and the corresponding three-dimensional projections of three HA samples. Symbols have the same significance as in Fig. 2.

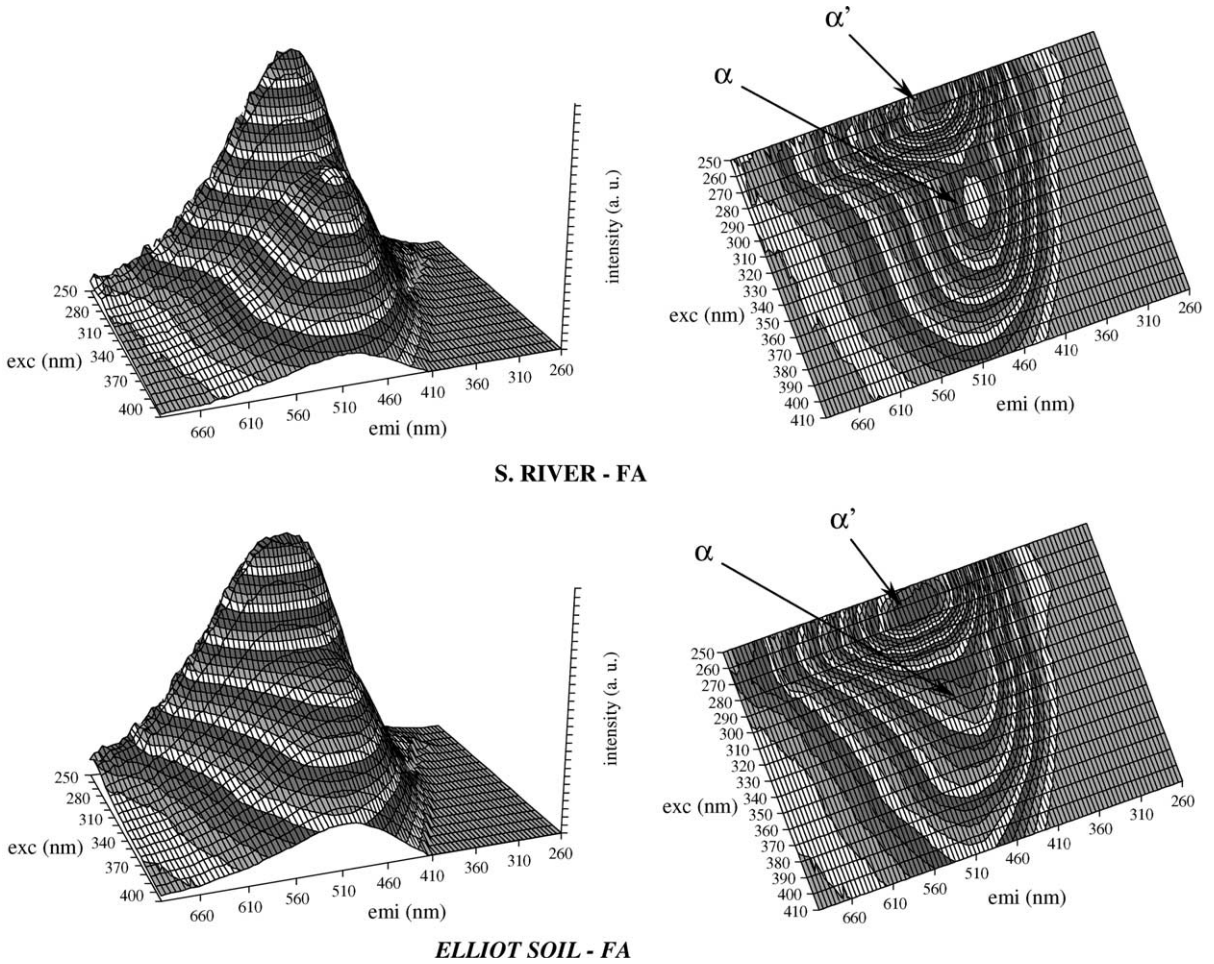

Fig. 4. EEM fluorescence diagrams and the corresponding three-dimensional projections of two IHSS standard FA.

molar mass, the more spread the fluorescence excitation spectra towards longer wavelengths (Belin et al., 1993). It has been also suggested, following pH variations in FA solutions, that the 300–350 nm region in the excitation spectra is dominated by chromophores with high carboxylic groups content, while structures containing phenolic groups act between 350 and 400 nm (Silva, 1996). Differences observed between FA and HA EEM spectra, could be equally explained by these two arguments. In fact, the higher aromatic condensation in HA overlaps electronic transitions, producing an excitation spectrum less contrasted than that of fulvic acids. Also, with respect to the acidic contents, the carboxylic group average concentration is, for these FA, higher than that of HA by as much as a factor of 1.5 (Fernandes et al., 2004).

FA fluorescence intensities are higher than those of HA at identical concentrations (Tables 1–3). High fluorescence intensity is, in general, associated with low molar mass components, low condensation and low aromatic degree (Miano et al., 1988; Senesi et al., 1991). The greater proximity of aromatic chromophores and, consequently the greater probability of deactivation of the excited states by internal quenching in high molar mass molecules, like HA, diminishes the fluorescence intensity (Senesi, 1990) and shifts the maxima to higher wavelengths. These trends corroborate the results relative to the peak positions as well as to recurrent data presented in the literature about the differences between the molar masses of FA and HA (Aiken and Gillam, 1989).

For FA the α and α′ peak relative intensities change slightly from one sample to another. Comparing the samples collected from the two sites in the Ratones Mangrove, for example, it can be noticed that the α peak is more apparent in the far-from-sea (Fig. 8: RME 2A, 0-10 cm) than in the near-to-sea samples (Fig. 2: RME 1A, 0–10 cm). For natural waters, the ratio between

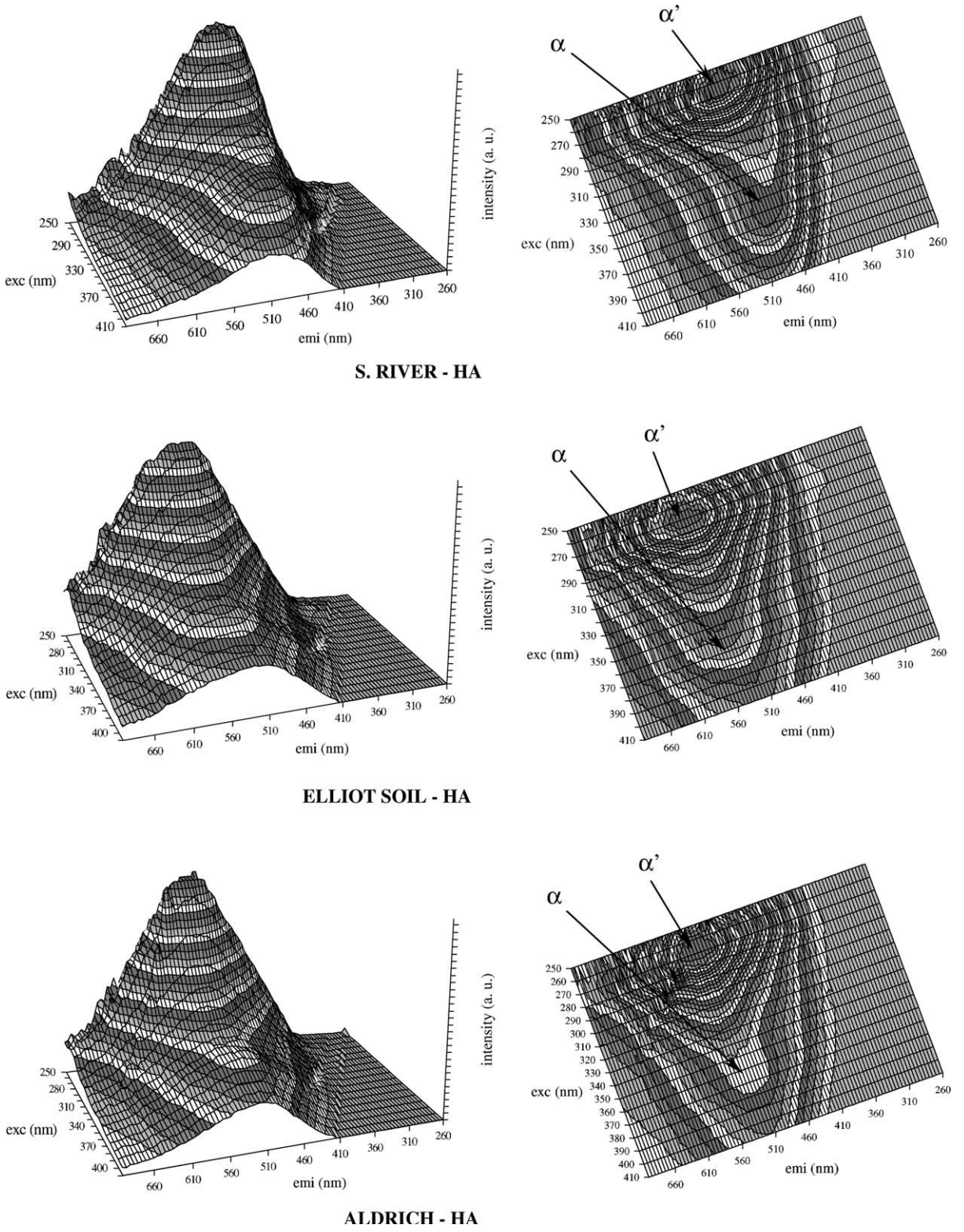

Fig. 5. EEM fluorescence diagrams and the corresponding three-dimensional projections of two IHSS standard and of the Aldrich HA.

Table 1
Fluorescence data of the FA samples

Samples	Fluorophore[a]	$\lambda_{ex}/\lambda_{em}$ (nm)	Intensity (cps)	Ratio α′/α
FA—UBM	α′	255/454	1 996 569	
	α	310/440	1 244 105	1.60
	γ	275/320	482 355	
FA—MVI	α′	255/458	2 418 098	
	α	310/438	1 570 061	1.54
	γ	275/320	440 214	
FA—PLN 4	α′	255/454	3 825 992	
	α	310/442	2 499 315	1.53
	γ	–	–	
FA—PLN 7	α′	255/456	4 094 953	
	α	310/440	2 544 534	1.61
	γ	–	–	
FA—RME 1A	α′	260/458	3 412 590	
	α	310/444	1 967 048	1.73
	γ	270/330	426 473	
FA—RME 1B	α′	260/460	3 365 502	
	α	310/444	2 029 827	1.66
	γ	270/330	380 699	
FA—RME 1C	α′	260/465	3 339 002	
	α	310/442	1 822 118	1.83
	γ	270/325	438 926	
FA—RME 2A	α′	255/455	2 155 908	
	α	315/450	1 601 025	1.35
	γ	270/305	1 722 715	
FA—RME 2B	α′	255/460	2 872 295	
	α	315/450	1 873 647	1.53
	γ	270/305	991 619	
FA—RME 2C	α′	255/455	2 796 313	
	α	315/445	1 708 481	1.64
	γ	270/310	746 247	

[a] According to Parlanti et al. (2000) denominations.

these two peak intensities has been employed to distinguish between fluorescent OM from terrestrial and marine environments with the highest values being measured in open-sea waters due to the reduced contribution of the α fluorophores in these environments (Sierra et al., 1994; Coble, 1996; Sierra et al., 1997). The α′/α ratio values for all samples are shown in Tables 1–3. The higher influence of the α fluorophores on FA than on HA fluorescence is confirmed by these values. From these data, however, it is not possible to infer conclusively about the samples origin, as in the case of natural waters, because general trends are not observed. The terrestrial Elliot soil FA, for example, showed a α′/α value which is higher than the coastal marine UBM and MVI samples. Special cases are the estuarine FA whose α′/α values are clearly higher for the samples collected near to sea (RME 1A, 1B and 1C) than for the samples collected far from the sea (RME 2A, 2B and 2C). Also, for these FA, it can be observed that, in both sites, the upper-layer samples present lower values than the deep-layer samples. Such increasing in the ratio with depth might be a consequence of the OM aging, humification leading to the decaying of the α fluorophores relatively to the α′ fluorophores. This hypothesis agrees with the fact that the α′/α ratio values are higher for HA than for FA. In natural waters, the α peak has been associated with terrestrial (e.g. lignin-derivatives) contributions (Sierra et al., 1994, 1997; Coble, 1996) as well as to degradation products of purely marine origin (Parlanti et al., 2000). According to our data, in extracted HS, the extent of its contribution to the longer wavelength emission fluorescence signal seems be equally strongly dependent on the humification degree of the samples.

Besides these two main fluorescence regions, most of samples presented a third signal. For FA, it is located within the range *Ex*/*Em* = 270–275 nm/305–320 nm and for HA in the range *Ex*/*Em* = 270–275 nm/330–345 nm (Figs. 2, 3 and 8 and Tables 1–3). This signal is present in HS diagrams with varied intensities. Whereas for most samples it is more like a shoulder,

Table 2
Fluorescence data of the HA samples

Samples	Fluorophore[a]	$\lambda_{ex}/\lambda_{emi}$ (nm)	Intensity (cps)	Ratio α′/α
HA—UBM	α′	265/525	977896	
	α	360/525	352305	2.77
	γ	275/345	175381	
HA—MVI	α′	265/515	1471348	
	α	360/515	532330	
	γ	270/330	1114432	2.76
	β	320/425	467098	
HA—PLN 4	α′	265/525	1652147	
	α	360/520	558015	2.96
	γ	275/340	135150	
HA—PLN 7	α′	265/520	1907765	
	α	360/515	668804	2.85
	γ	275/345	147456	
HA—RME 1A	α′	265/530	1797255	
	α	360/525	630096	2.85
	γ	275/335	164730	
HA—RME 1B	α′	265/530	1966142	
	α	360/530	705913	2.79
	γ	275/345	151135	
HA—RME 1C	α′	265/530	1925831	
	α	360/525	687376	2.80
	γ	275/345	155777	
HA—RME 2A	α′	265/525	1100604	
	α	360/515	405763	
	γ	275/335	150301	2.71
	β	320/430	372737	
HA—RME 2B	α′	265/525	1552621	
	α	360/520	552472	2.81
	γ	275/345	176268	
HA—RME 2C	α′	265/515	1359497	
	α	360/515	475920	
	γ	275/340	229581	2.86
	β	320/425	426628	
HA—Aldrich	α′	265/525	2130731	
	α	360/520	673352	3.16
	γ	–	–	

[a] According to Parlanti et al. (2000) denominations.

for the FA fractions extracted from Site 2 in the Ratones Mangrove (RME 2A, 2B and 2C) it is very significant (Fig. 8). It is, conversely, absent and very weak in the FA and HA plots respectively of the lake (PLN) samples (Figs. 2 and 3). The Aldrich HA does not present this peak and in the IHSS standard HS diagrams only a very slight fluorescence vestige can be observed in this range (Figs. 4 and 5). In the case where it is prominent this peak appears relatively separated from the other features. For natural waters, fluorescence signals within this range have usually been attributed to protein-derived compounds being designated as B or γ (tyrosine and/or protein-like peak with $\lambda_{em} \sim 310$ nm) and as *T* or δ (tryptophan and/or protein-like peak, with $\lambda_{em} \sim 340$ nm) (Coble, 1996; Parlanti et al., 2000). The comparison of our data with these studies as well as with those reported by Determann et al. (1998) and Mayer et al. (1999) indicates that the signal detected in our HS could, effectively be associated to the presence of these aromatic amino acids. Phenol exhibits a fluorescence excitation peak in this exact range, and, because of this, this feature has equally been associated with mono-aromatic phenolic compounds, which are also precursors for part of the future fluorescent OM (Ferrari and Mingazzini, 1995). It is not possible to distinguish between amino acids and mono-aromatic phenolic compounds signals in the EEM diagrams. However, as this signal is usually encountered in seawater samples (Ferrari and Mingazz-

Table 3
Fluorescence data of the IHSS samples

Samples	Fluorophore[a]	$\lambda_{ex}/\lambda_{emi}$ (nm)	Intensity (cps)	Ratio α'/α
Fulvic acids				
Suwannee River Fulvic Acid (1S101F)	α'	255/455	2563467	1.61
	α	320/450	1590053	
Elliot Soil Fulvic Acid (1S102F)	α'	265/475	4168873	1.93
	α	325/440	2159418	
Humic acids				
Suwannee River Humic Acid (1S101H)	α'	260/485	1459599	2.12
	α	330/470	689360	
Elliot Soil Humic Acid (1S102H)	α'	270/550	2450461	2.63
	α	360/560	930884	

[a] According to Parlanti et al. (2000) denominations.

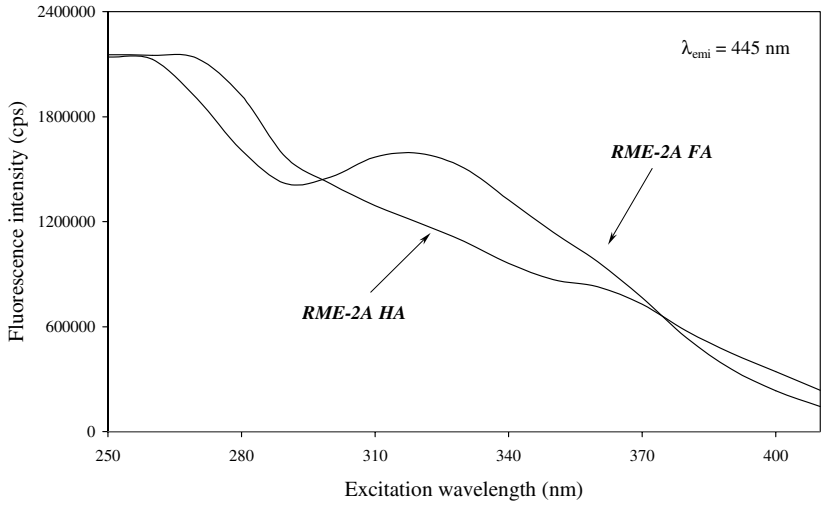

Fig. 6. Single-scan excitation spectra of a FA and a HA samples from Ratones Mangrove (Site 2, first layer) recorded using a $\lambda_{emi} = 445$ nm.

ini, 1995; Coble, 1996; Parlanti et al., 2000) and, in the present study, it is hardly detected in the samples from exclusively terrestrial sources, we will also assume a protein origin for this peak in the following discussion.

At a first view, vis-à-vis the peak maxima, tyrosine (γ) seems to be the major contributor to FA whereas tryptophan (δ) seems to be mainly responsible for the HA protein-like peaks. However, as has been shown in previous studies, intact proteins containing both tyrosine and tryptophan residues are generally dominated by tryptophan fluorescence due to the higher quantum yield of the latter (Determann et al., 1998). Determann et al. (1998), for example, investigated the fluorescence properties of a series of marine bacteria and phytoplankton cultures and observed that the tryptophan signal was dominant. They also showed that in denatured proteins tryptophan emission is blue-shifted relatively to its regular emission signal exhibiting, in this case, a peak centred at 305 nm which may overlap the tyrosine signal. During extraction and purification, HS are strongly handled being submitted to extreme acidic and alkaline conditions, among other procedures. After such treatment it seems highly unlikely that proteins would remain in their intact form. Hence, tryptophan or its metabolites might be mainly responsible for the fluorescence signal observed in all samples. The δ designation will subsequently employed.

The peaks in this range of the fluorescence spectra and EEM diagrams have been used as markers to estimate biological activity and the different stages of the biological production in coastal zones (Mayer et al., 1999; Parlanti et al., 2000). According to Parlanti et al. (2000) the more prominent the γ peak the earlier the stage of degradation of the freshly produced biological material, in natural waters. Most of our samples were from highly productive environments (estuaries and

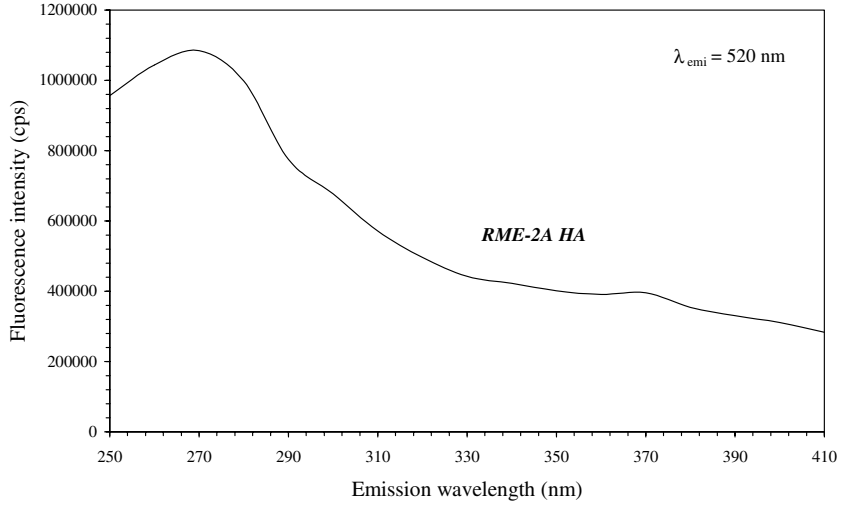

Fig. 7. Single-scan excitation spectra of a HA sample from Ratones Mangrove (Site 2, first layer) recorded using a λ_{emi} = 520 nm.

coastal zones), with considerably high sedimentation rates, and the signals for the presence of recent OM in these extracted HS confirms its relatively low humification degree. Actually, from the elemental, functional and spectral properties of this set of samples (Fernandes et al., 2004; Giovanela et al., 2004; Sierra et al., 2004) it was also inferred that they preserve significant moieties of the source materials. The reasons for the presence of a stronger protein-like signal in the RME-FA (Site 2) than in the other samples is not clear but it is interesting to observe the decreasing of its relative intensity from upper to lower sediment layers (Fig. 8). Coble (1996) also detected protein-like fluorescence in sediment pore waters, with the greatest concentrations being detected near the sediment-water interface. The occurrence of protein derived materials in FA and practically none in HA, in spite of the fact that the former were the more extensively handled during the extraction procedures, might be due to protein water-solubility characteristics, which might follow the FA patterns. The attributing of this signal to phenol-like structures, on the other hand, could make easier the explanation for the reasons for its greater manifestation in the samples from Site 2 in Ratones Mangrove, which, in comparison with other marine and estuarine samples presented the most evident signals of terrestrial OM influence (Giovanela et al., 2004; Sierra et al., 2004). The presence of unhumified compounds whether protein-like and/or phenol-like, in these samples is a sign of their lower aging relatively to the others, and does not invalidate the discussion above.

In spite of being the samples that gave the most evident infrared signals of the presence of polypeptides (Sierra et al., 2004), the lake (PLN) HA samples do not exhibit the protein-like fluorescence (Fig. 3) indicating that its protein residues are predominantly aliphatic, so endorsing the aliphatic nature of the material as a whole.

Finally, a fourth and barely perceptible shoulder appears at around *Ex*/*Em* = 320 nm/425 nm in a few HA diagrams. It is best seen in the EEM diagrams of the marine HA (MVI) and of the three HA from Site 2 in Ratones Mangrove (RME 2A, 2B and 2C) (Figs. 3 and 9). EEM fluorescence signals in this range have been associated with the presence of marine humic-like compounds being designed as β (Sierra et al., 1994; Parlanti et al., 2000) or M (Coble, 1996) components. These components have been indicated as being responsible for the blue-shift observed moving from fresh to marine environments both in single-scan and in EEM fluorescence of natural waters (Sierra et al., 1994, 1997; Coble, 1996; Parlanti et al., 2000). Here again, from the overall view given by the EEM plots it becomes clear why the 313 nm excitation wavelength has been so sensitive in detecting differences in the single-scan fluorescence maxima of natural waters (Sierra et al., 1994, 1997). Spectra obtained with λ_{ex} around this value represent essentially the emission of the α plus β fluorophores, the blue- or red-shifts being dependent on the relative abundance of each one in each sample.

In natural waters EEM diagrams the β signal has been observed in association with the protein-like, mainly the γ, peaks suggesting that both components have the same biological origin, with the γ components being the precursors for the β components (Parlanti et al., 2000). Hence, to find β component signals in the samples from Site 2 in Ratones Mangrove is not surprisingly since the FA samples with the most evident γ (or δ) signals on their diagrams also come from this collection point. The absence of the β peak from the FA diagrams can be attributed to both, its solubility characteristics

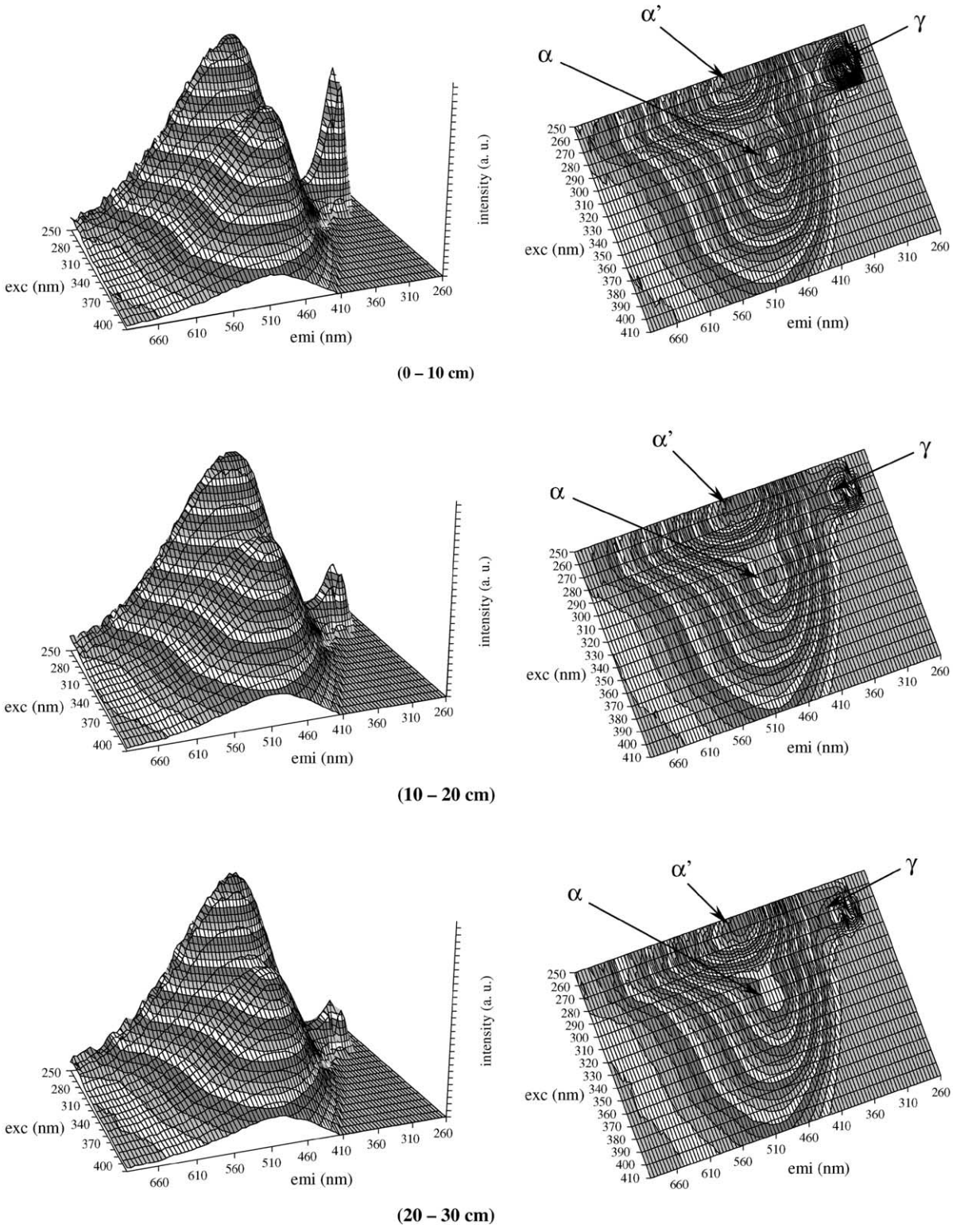

Fig. 8. EEM fluorescence diagrams and the corresponding three-dimensional projections of estuarine FA samples (Ratones Mangrove, Site 2, far-from-sea) from three different sediment depths.

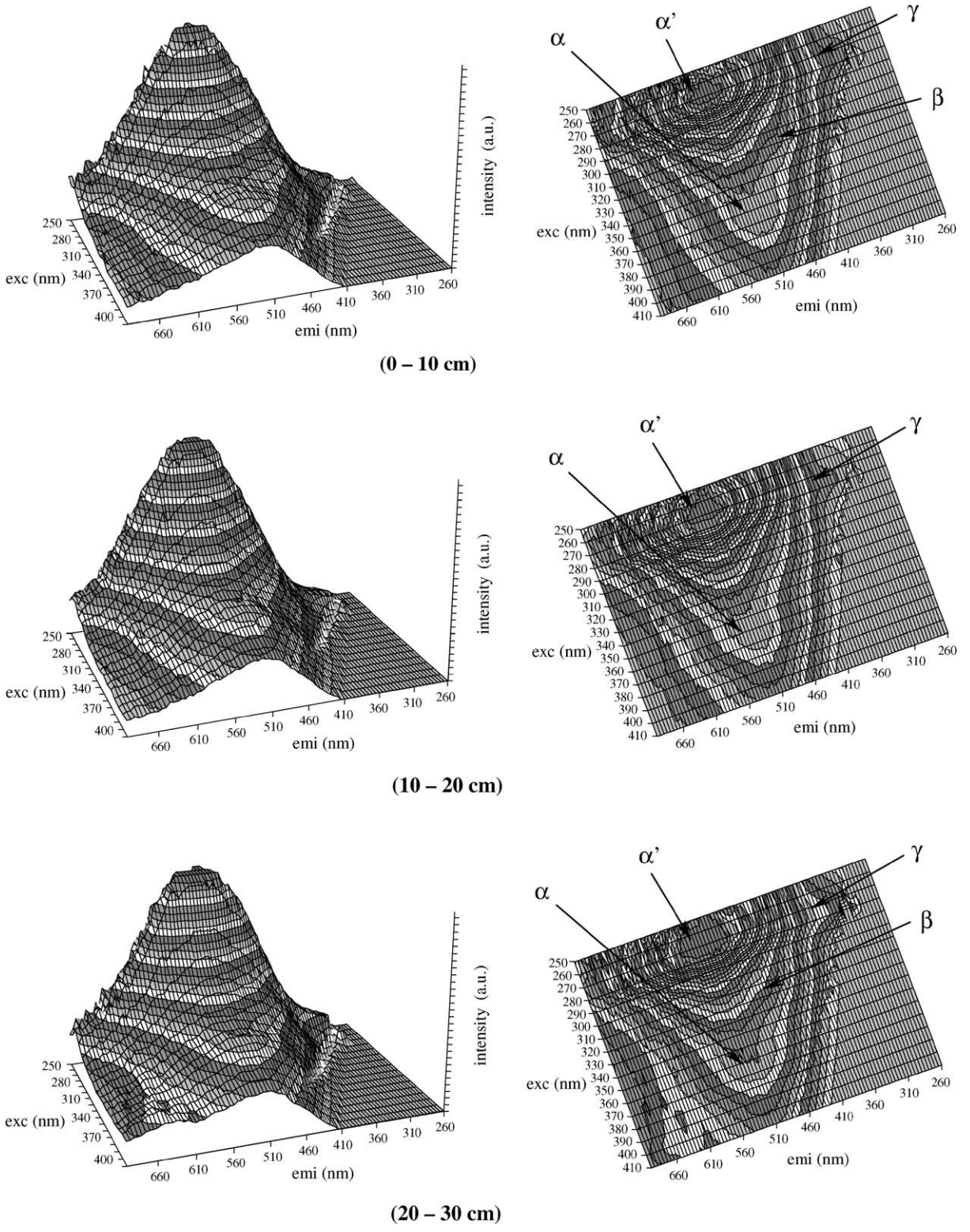

Fig. 9. EEM fluorescence diagrams and the corresponding three-dimensional projections of estuarine HA samples (Ratones Mangrove, Site 2, far-from-sea) from three different sediment depths.

which can follow the HA patterns and also to the fact that, in FA the α peak is very intense overlapping the β emission. In HA, the emission ranges are red-shifted to above 520 nm making more room for the β peak appearance. In fact, except for the lake HS, the Aldrich HA and the IHSS samples, the β fluorophore should be present to varied extents in all of the other samples but its signal might be overlapped by the stronger fluorescence (mainly in FA diagrams) of the humic-like (α) peak.

Some minor differences in fluorescence intensities and in peak positions from one sample to another are also apparent (Tables 1–3) suggesting that there are minor differences in HS composition.

3.2. Synchronous spectra

Synchronous excitation has recurrently been used in HS and natural water fluorescence studies (Cabaniss and Shuman, 1987; Miano et al., 1988; Miano and Senesi, 1992; Esteves da Silva and Machado, 1995; Ferrari and Mingazzini, 1995; Lombardi and Jardim, 1997) because in this fluorescence mode the spectra are, usually, more structured than the corresponding excitation and emission spectra. As a matter of fact, in the present study, as we obtained the complete fingerprint of HS by EEM plots, it should be unnecessary to make use of other fluorescence techniques to seek further "hidden" fluorophores. However, the following data and its discussion intend to show the real shapes of HS synchronous spectra as well as to explain the reasons for those shapes.

The synchronous technique consists of varying simultaneously both excitation and emission wavelengths while keeping a constant wavelength interval $\Delta\lambda$ between them. The synchronous signal will be observed only when fluorescence excitation and emission can both occur over the $\Delta\lambda$ selected (Vo-Dinh, 1978). This makes the shape and the bandwidth of a synchronous fluorescence spectrum, strong functions of the $\Delta\lambda$ selected. The selectivity toward any given component in a mixture can be enhanced by using a $\Delta\lambda$ that corresponds to the wavelength interval between the excitation and the emission maxima for that component (Vo-Dinh, 1978). Consequently, concerning HS, the principal difficulty involved in this technique, is to find the ideal $\Delta\lambda$ interval, i.e. the value that will produce the most representative spectra of each fluorophore, in each sample. In fact, such a condition seems impossible to achieve because the individual characteristics of humic fluorophores are not known. Furthermore, as can be seen in the HS EEM plots, the emission maxima shift to longer or shorter wavelengths according to the excitation wavelength employed. Hence, to have a complete picture of each sample several $\Delta\lambda$ should be tested before each study. Miano and Senesi (1992) investigated the effect of varying $\Delta\lambda$ on the shape of the synchronous-scan spectra of a series of FA and HA and observed that a value of $\Delta\lambda = 18$ nm produced the best overall spectral resolution. Most studies on HS synchronous technique have, on the other hand, employed a $\Delta\lambda = 20$ nm (Cabaniss, 1992; Machado et al., 1994; Silva et al., 1994; Lombardi and Jardim, 1997).

The effect of varying $\Delta\lambda$ on the shape of the HS synchronous spectra can be better understood through the EEM diagrams. Figs. 10 and 11 show the EEM plots of, respectively, a FA and a HA sample from the first layer of Site 2 in Ratones Mangrove (RME-2A). These samples were chosen to illustrate this discussion because they exhibited the greatest number of features in their EEM diagrams. Five lines are traced diagonally on each diagram, each one corresponding to a spectral range scanned by the synchronous mode, with $\Delta\lambda$ values of 20, 50, 80, 100 and 150 nm. Moving across these lines from the lowest to the highest excitation wavelengths it becomes comprehensible both, the shape of the corresponding synchronous spectra and the fact that these plots cover only partially numerous spectral possibilities. Below each diagram, for each sample, the five corresponding synchronized fluorescence spectra are represented. The λ_{ex} limits of 250–410 nm on these synchronous spectra are the same as in the EEM plots and, because of this, for HA, whose EEM peaks are red-shifted, the second range is not completely covered, showing, consequently, a poorer definition. Two peak ranges are, in general, observed in these plots, below and above 300 nm, respectively. The first peak, around 275 nm appears for both FA and HA being more structured in the former. From the EEM diagrams it can be seen that this range corresponds to the range of the protein- and/or phenol-like (i.e. the γ or δ) peaks. Ferrari and Mingazzini (1995) using the synchronous technique ($\Delta\lambda = 25$ nm) have detected this peak in seawater samples and also related its incidence to recent fluorescent OM biological production. With an off-set of 20 nm, for most of our samples, these are the unique fluorophores that can be well distinguished in synchronous spectra. Using intermediate $\Delta\lambda$ (50 and 80, for example) the γ (or δ) and the α peaks are both evidenced (at least in FA). Obviously these data will change from sample to sample since they will depend on how large the spectral range is in each case. The $\Delta\lambda = 50$ nm was chosen to compare these synchronous spectra with previous studies (Sierra et al., 1994). Observe that with this off-set (and also with off-sets of 80 an 100 nm) the RME-2A HA synchronous spectrum presents an extra feature at around 320 nm, corresponding to the excitation range of the β fluorophores. These fluorophores are typical of marine humic-like material (Parlanti et al., 2000) and once more, the overall view given by the EEM plots explains why this off-set value had been the most accurate at producing the more structured synchronous spectra of marine and estuarine waters (Sierra et al., 1994). A

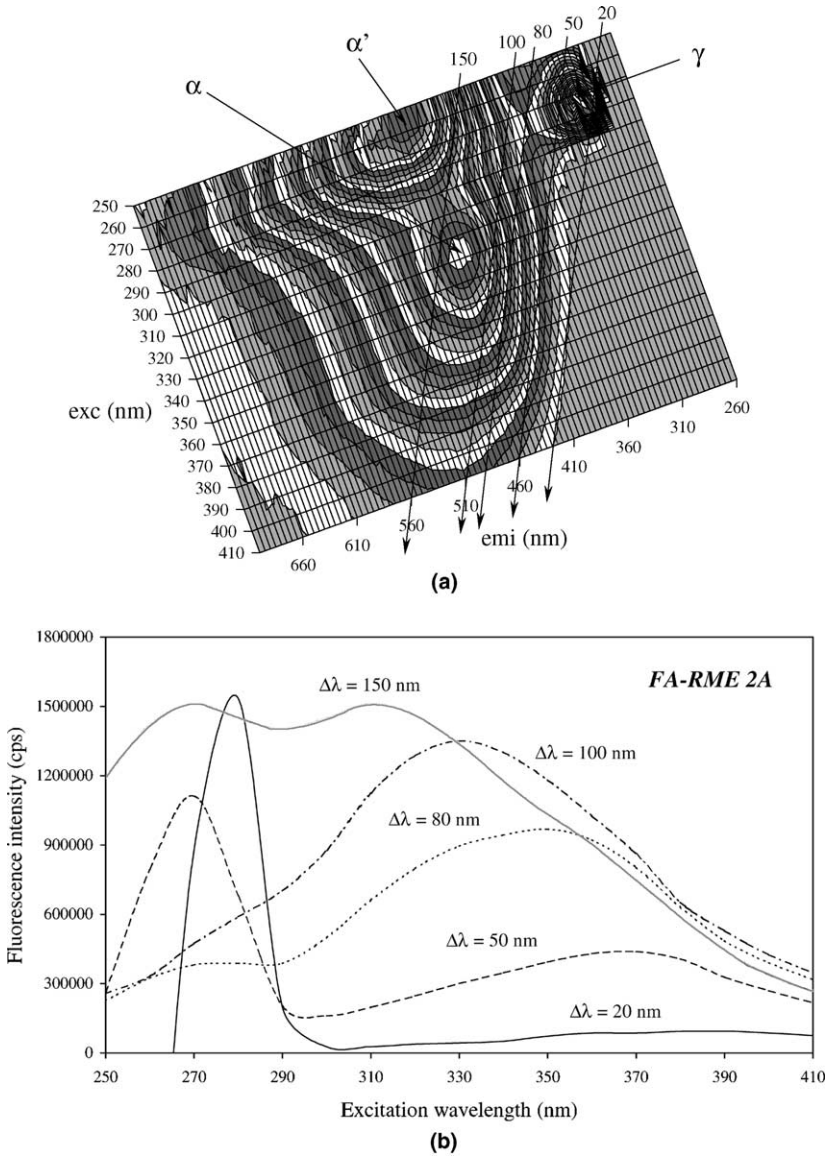

Fig. 10. (a) EEM fluorescence diagram of an estuarine FA sample (Ratones Mangrove, first layer, Site 2, far-from-sea). The lines traced diagonally across the diagram indicate the spectral ranges covered by the synchronous mode using four different $\Delta\lambda$ values: 20, 50, 80, 100 and 150 nm. (b) Synchronous spectra recorded using the $\Delta\lambda$ corresponding to the five lines on the EEM diagram above.

$\Delta\lambda$ = 150 nm encompasses partially the α' and totally the α peaks for these samples as can be seen in the corresponding synchronized spectrum (mainly for FA). To get a better register of the α' peak, on the other hand, a still larger $\Delta\lambda$ would be needed.

3.3. Fluorophores distinction

Attempts have been made to point out individual chemical components that could be at the origin of the humic fluorescence and a series of compounds potentially responsible for such signals have been listed (Senesi, 1990 and references therein). These compounds include hydroxybenzoic acids and other substituted phenolic units originating from lignin, hydroxycoumarin-like structures, Schiff-base systems and chromone, xanthone and/or quinoline derivatives originated from degraded plant materials. These fluorescence precursors exhibit λ_{ex}(max) within the range 310–410 nm and λ_{em}-(max) within the range 410–490 nm (Senesi, 1990 and references therein) and might, effectively, be at the origin of the signals centred at *Ex*/*Em* = 260 nm/460 nm (the α' peak) and/or at *Ex*/*Em* = 310 nm/440 nm (the α peak) for FA and natural waters. Also the protein-like (γ

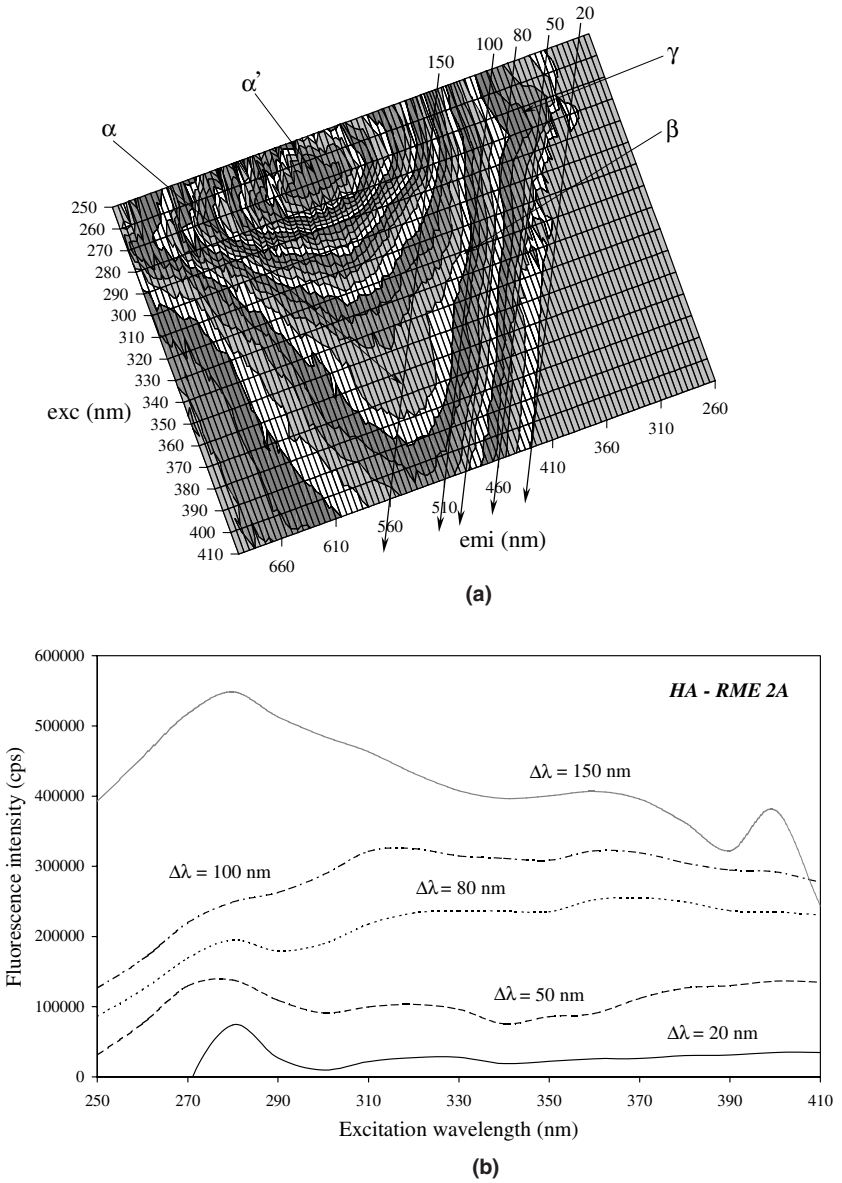

Fig. 11. (a) EEM fluorescence diagram of an estuarine HA sample (Ratones Mangrove, first layer, site 2, far-from-sea). The lines traced diagonally across the diagrams indicate the spectral ranges covered by the synchronous mode using four different $\Delta\lambda$ values: 20, 50, 80, 100 and 150 nm. (b) Synchronous spectra recorded using the $\Delta\lambda$ values corresponding to the four lines on the EEM diagram above.

and δ) peaks, have been related to tyrosine and/or tryptophan fluorescence (Coble, 1996; Determann et al., 1998; Parlanti et al., 2000). None of the listed compounds, however, exhibits λ_{em} as long as those observed here for HA. Only a greatly conjugated system of these and other compounds could produce such a batochromic effect in fluorescence emission. Even for higher aromatic structures such as fluoranthene, dibenzo-perylene, and dibenzo-anthracene, for example, the λ_{em} are usually situated below 500 nm (Van Duuren, 1960). Chlorophyll-a degradation products couldn't be responsible for this signal either since their fluorescence maxima are situated above 650 nm (French, 1960). HS EEM diagrams represent, indeed, the sum of the contribution of many different fluorophores and in spite of the overall view given by this technique the question of the fluorophores responsible for HS, principally HA fluorescence, remains unanswered. The combined spectral signature of these contributions is, however, definitively established in this study.

4. Concluding remarks

The whole spectral maps (λ_{ex} from 250 to 410 nm and λ_{em} from 260 to 700 nm) of FA and HA are, in general terms, composed of four main peak ranges. Comparison between the *Ex*/*Em* pairs of these peaks and those published in related studies allowed their association with the α' (or C), α (or A), β (or M) and γ/δ (*M*/*T*) fluorophores already detected in natural water spectra diagrams. Samples from marine and estuarine media are richer in spectral features than samples from exclusively terrestrial media. The OM aging also has an influence on the variety of the EEM signals, the older the samples the poorer their spectral features.

The α' and α peaks were present in all samples independently of their origin. Their *Ex*/*Em* pair values in FA indicate that this humic fraction is chiefly responsible for natural waters fluorescence. The β peak was observed in a few samples, mainly HA, from marine and estuarine environments but its appearance depends on the balance between its magnitude and that of the α peak. The δ (or γ) peak, which is attributed to protein-, mainly tryptophan-like materials, appears in most samples but it is also more marked in marine and estuarine FA. Single-scan excitation and synchronous spectra, which were recorded for all samples, confirm all these findings.

Overall, the data showed that in spite of the strong handling to which HS are submitted during extraction and purification procedures their spectral signals maintain a certain identity that allows the identification of their origin, EEM fluorescence being an efficient tool to assess both the OM sources (terrestrial or marine) and the aging of the extracted material.

Finally, careful analysis of these data showed that in the cases where the fluorescence equipment available does not have the technical requirements to perform a complete scanning like in EEM diagrams, the single-scan excitation and emission spectra combined with synchronous spectroscopy can satisfactorily be used to scrutinize OM sources in HS, provided that appropriate λ_{ex}, λ_{em} and $\Delta\lambda$ are employed.

Acknowledgments

This work was supported by the Conselho Nacional de Pesquisa e Desenvolvimento (CNPq, Brazil) and the Coordenação de Aperfeiçoamento de Pessoal de Nível Superior (CAPES, Brazil).

References

Aiken, G.R., Gillam, A.H., 1989. Determination of molecular weights of humic substances by collogative property measurements. In: Hayes, M.H.B., MacCarthy, P., Malcolm, R.L., Swift, R.S. (Eds.), Humic Substances II, in search of structure. John Wiley & Sons Ltd, Chichester.

Baker, A., 2001. Fluorescence excitation–emission matrix characterization of some sewage-impacted rivers. Environ. Sci. Technol. 35, 948–953.

Belin, C., Quellec, C., Lamotte, M., Ewald, M., Simon, Ph., 1993. Characterization by fluorescence of the dissolved organic matter in natural water. Application to fractions obtained by tangential ultrafiltration and XAD resin isolation. Environ. Technol. 14, 1131–1144.

Cabaniss, S.E., 1992. Synchronous fluorescence spectra of metal–fulvic acid complexes. Environ. Sci. Technol. 26, 1133–1139.

Cabaniss, S.E., Shuman, M.S., 1987. Synchronous fluorescence spectra of natural waters: tracing sources of dissolved organic matter. Mar. Chem. 21, 37–50.

Chen, J., LeBoeuf, E.J., Dai, S., Gu, B., 2003. Fluorescence spectroscopic studies of natural organic matter fractions. Chemosphere 50, 639–647.

Coble, P.G., 1996. Characterization of marine and terrestrial DOM in seawater using excitation–emission matrix spectroscopy. Mar. Chem. 51, 325–346.

Del Castillo, C.E., Coble, P.G., Morell, J.M., Lopez, J.M., Corredor, J.E., 1999. Analysis of the optical properties of the Orinico River plume by absorption and fluorescence spectroscopy. Mar. Chem. 66, 35–51.

Determann, S., Lobbes, J.M., Reuter, R., Rullkötter, J., 1998. Ultraviolet fluorescence excitation and emission spectroscopy of marine algae and bacteria. Mar. Chem. 62, 137–156.

Esteves da Silva, J.C.G., Machado, A.A.S.C., 1995. Evolving factor analysis of synchronous fluorescence spectra of humic substances in the presence of Cu(II). Chemometr. Intell. Lab. Syst. 27, 115–128.

Ewald, M., Belin, C., Berger, P., Weber, J.H., 1983. Corrected fluorescence spectra of fulvic acids isolated from soil and water. Environ. Sci. Technol. 17, 201–504.

Fernandes, A.N., Giovanela, M., Soriano-Sierra, E.J., Sierra, M.M.D., 2004. Acidity data on humic substances from distinct environments: methodology considerations. J. Coastal Res. SI, 39, in press.

Ferrari, G.M., Mingazzini, M., 1995. Synchronous fluorescence spectra of dissolved organic matter (DOM) of algal origin in marine coastal systems. Mar. Ecol. Progr. Series 125, 305–315.

French, C.S., 1960. The chlorophylls in vivo and in vitro. In: Ruhland, W. (Ed.), Encyclopedia of Plant Physiology, Vol. 5/1. Berlin, Springer, pp. 252–297.

Fukushima, M., Tanaka, S., Nakayasu, K., Sasaki, K., Nakamura, H., Tatsumi, K., 1997. Anal. Sci. 13, 1011–1015.

Giovanela, M., Parlanti, E., Soldi, M.S., Soriano-Sierra, E.J., Sierra, M.M.D., 2004. Elemental compositions, FT-IR spectra and thermal behavior of sedimentary fulvic and humic acids from aquatic and terrestrial environments. Geochem. J. 38, 255–264.

IHSS home page: http://www.ihss.gatech.edu/.

Lombardi, A.T., Jardim, W.F., 1997. Synchronous-scan fluorescence and the complexation of copper (II) ions by humic substances. J. Braz. Chem. Soc. 8, 1–6.

Machado, A.A.S.C., Esteves da Silva, J.C.G., Maia, J.A.C., 1994. Multi-wavelength analysis of synchronous fluores-

cence spectra of the complexes between a soil fulvic acid and Cu(II). Anal. Chim. Acta 292, 121–132.

Malcolm, R.L., MacCarthy, P.M., 1986. Limitations in the use of commercial humic acids in water and soil research. Environ. Sci. Technol. 20, 904–911.

Mattews, B.J.H., Jones, A.C., Theodorou, N.K., Tudhope, A.W., 1996. Excitation–emission-matrix fluorescence spectroscopy applied to humic acid bands in coral reefs. Mar. Chem. 55, 317–332.

Mayer, L.M., Schick, L.L., Loder III, T.C., 1999. Dissolved protein fluorescence in two Maine estuaries. Mar. Chem. 64, 171–179.

Miano, T.M., Senesi, N., 1992. Synchronous excitation fluorescence spectroscopy applied to soil humic substances chemistry. Sci. Total Environ. 117/118, 41–51.

Miano, T.M., Sposito, G., Martín, J.P., 1988. Fluorescence spectroscopy of humic substances. Soil Sci. Soc. Am. J. 52, 1016–1019.

Mobed, J.J., Hemmingsen, S.L., Autry, J.L., MacGown, L.B., 1996. Fluorescence characterization of IHSS humic substances: total luminescence spectra with absorbance correction. Environ. Sci. Technol. 30, 3061–3065.

Mopper, K., Schultz, C.A., 1993. Fluorescence as a possible tool for studying the nature and water column distribution of DOC components. Mar. Chem. 41, 229–238.

Mounier, S., Patel, N., Quilici, L., Benaim, J.Y., Benamou, C., 1999. Fluorescence 3D de la matière organique dissoute du fleuve Amazone (Three-dimensional fluorescence of the disolved organic carbon in the Amazon river). Water Res. 33, 1523–1533.

Parlanti, E., Morin, B., Vacher, L., 2002. Combined 3D-spectrofluorimetry, high performance liquid chromatography and capillary electrophoresis for the characterization of dissolved organic matter in natural waters. Org. Geochem. 33, 221–236.

Parlanti, E., Wörz, K., Geoffroy, L., Lamotte, M., 2000. Dissolved organic matter fluorescence spectroscopy as a tool to estimate biological activity in a coastal zone submitted to anthropogenic inputs. Org. Geochem. 31, 1765–1781.

Patel-Sorrentino, N., Mounier, S., Benaim, J.Y., 2002. Excitation–emission fluorescence matrix to study pH influence on organic matter fluorescence in the Amazon basin rivers. Water Res. 36, 2571–2581.

Senesi, N., 1990. Molecular and quantitative aspects of the chemistry of fulvic acid and its interactions with metal ions and organic chemicals. Part II. The fluorescence spectroscopy. Anal. Chim. Acta 232, 77–106.

Senesi, N., Miano, T.M., Provenzano, M.R., Brunetti, G., 1991. Characterization, differentiation, and classification of humic substances by fluorescence spectroscopy. Soil Sci. 152, 259–271.

Sierra, M.M.D., Donard, O.F.X., Lamotte, M., 1997. Behaviour of dissloved fluorescent organic matter during estuarine mixing. Mar. Chem. 58, 51–58.

Sierra, M.M.D., Donard, O.F.X., Lamotte, M., Belin, C., Ewald, M., 1994. Fluorescence spectroscopy of coastal and marine waters. Mar. Chem. 47, 127–144.

Sierra, M.M.D., Giovanela, M., Soriano-Sierra, E.J., 2000. Fluorescence properties of well-characterized sedimentary estuarine humic compounds and surrounding pore waters. Environ. Technol. 21, 979–988.

Sierra, M.M.D., Giovanela, M., Esteves, V.I., Duarte, A.C., Fransozo, A., Parlanti, E., 2004. Structural description of fulvic and humic acids from coastal and terrestrial environments using elemental analysis, FT-IR and ^{13}C-solid state NMR data. J. Coast. Res. SI, 42, in press.

Silva, M.R., 1996. Estudos potenciométricos e fluorimétricos dos equilíbrios ácido-básicos e da complexação de metais com o Obisdien e as substâncias húmicas. Contaminação pelos metais em sedimentos da Ilha de Santa Catarina (Brasil). PhD Thesis, Universidade Federal de Santa Catarina.

Silva, C.S.P.C.O., Esteves da Silva, J.C.G., Machado, A.A.S.C., 1994. Evolving factor analysis of synchronous fluorescence spectra of fulvic acids in the presence of aluminium. Appl. Spectrosc. 48, 363–371.

Swift, R.S., 1996. Organic matter characterization. In: Sparks, D.L. (Ed.), Methods of Soil Analysis. Soil Science Society of America, Madison, WI, pp. 1018–1020.

Van Duuren, B.L., 1960. The fluorescence spectra of aromatic hydrocarbons and heterocyclic aromatic compounds. Anal. Chem. 32, 1436–1442.

Vo-Dinh, T., 1978. Multicomponent analysis by synchronous luminescence spectrometry. Anal. Chem. 50, 396–401.